H.H.K. Xu[1,2,3]*, L. Zhao[1],
and M.D. Weir[1]

[1]Department of Endodontics, Prosthodontics and Operative Dentistry, University of Maryland Dental School, 650 West Baltimore Street, Baltimore, MD 21201, USA; [2]Center for Stem Cell Biology & Regenerative Medicine, University of Maryland School of Medicine, Baltimore, MD 21201, USA; and [3]Department of Mechanical Engineering, University of Maryland, Baltimore County, MD 21250, USA; *corresponding author, hxu@umaryland.edu

Stem Cell-Calcium Phosphate Constructs for Bone Engineering

ABSTRACT

While human bone-marrow-derived mesenchymal stem cells (hBMSCs) have been investigated, human umbilical cord mesenchymal stem cells (hUCMSCs) are a relatively new cell source. Little has been reported on hUCMSC encapsulation in scaffolds for bone tissue engineering. The objective of this study was to encapsulate hBMSCs and hUCMSCs in calcium phosphate cement (CPC) scaffolds for dental, craniofacial, and orthopedic applications. Stem-cell-encapsulating CPC construct with chitosan and fiber reinforcement reached the strength of cancellous bone, which was much stronger than previous injectable carriers for cell delivery. hUCMSCs and hBMSCs inside the constructs showed excellent viability and osteo-differentiation. The encapsulated hUCMSCs synthesized nearly three-fold more bone minerals than the hBMSCs *in vitro*. Hence, stem-cell-encapsulating CPC-chitosan-fiber construct may be promising for dental and orthopedic applications. This study indicated that the hUCMSCs were a potent alternative to the gold-standard hBMSCs, which may have a broad impact on regenerative medicine and dental tissue engineering.

INTRODUCTION

Seven million people suffer bone fractures annually in the United States, and musculoskeletal conditions cost $215 billion (Laurencin *et al.,* 1999; Praemer *et al*., 1999). The use of stem cells has immense potential for tissue engineering (Richardson *et al*., 2001; Sikavitsas *et al*., 2003; Mao *et al*., 2006; Mao, 2008). Human bone-marrow-derived mesenchymal stem cells (hBMSCs) can differentiate into osteoblasts, adipocytes, chondrocytes, myoblasts, neurons, and fibroblasts. They can be harvested from the patient, expanded *in vitro,* and combined with a scaffold to repair bone defects (Drury and Mooney, 2003; Benoit *et al*., 2007; Mao *et al*., 2007). However, hBMSCs require an invasive procedure to harvest and have lower self-renewal potential with aging. Recently, human umbilical cord mesenchymal stem cells (hUCMSCs) were differentiated into adipocytes, osteoblasts, chondrocytes, neurons, and other cells (Wang *et al*., 2004; Bailey *et al*., 2007; Baksh *et al*., 2007; Can and Karahuseyinoglu, 2007; Wang *et al*., 2009; Zhao *et al*., 2010). hUCMSCs have major advantages: (1) Umbilical cords can be collected at a low cost to serve as an inexhaustible stem cell source; (2) their harvest does not require the invasive procedure of hBMSCs and is without the controversies of embryonic stem cells (hESCs); (3) hUCMSCs exhibit high plasticity and developmental flexibility; and (4) hUCMSCs appear to cause no immunorejection. However, to date, little has been reported on hUCMSC encapsulation in scaffolds for bone engineering.

The lack of suitable scaffolds has hindered tissue engineering. Pre-formed scaffolds have difficulty in seeding cells deep into the scaffold and cannot be injected in minimally invasive surgeries. Currently available injectable carriers are mechanically weak. For example, it has been concluded that "Hydrogel scaffolds … do not possess the mechanical strength to be used in load-bearing applications" (Drury and Mooney, 2003). To date, an injectable, bioactive, and load-bearing scaffold for stem cell delivery is yet to be developed. The scaffold structure needs to be maintained to define the shape of the regenerated tissue. Mechanical properties are of crucial importance for the regeneration of load-bearing tissues such as bone, to withstand stresses to avoid scaffold fracture. Bioactive implants with bone-like calcium phosphate minerals can bond to native bone, because the minerals provide a preferred substrate for cell attachment and expression of osteoblast phenotype (LeGeros, 1993; Ducheyne and Qiu, 1999; Foppiano *et al*., 2004; Deville *et al*., 2006). However, for hydroxyapatite and other pre-formed bioceramics to fit into a bone cavity, the surgeon needs to machine the graft or carve the surgical site, leading to increases in bone loss, trauma, and surgical time (Laurencin *et al*., 1999).

In contrast, calcium phosphate cements (CPC) can be injected, or molded/shaped for esthetics in dental and craniofacial repairs, and then set *in situ* to form a bioactive scaffold that bonds to bone (Brown and Chow, 1986; Barralet *et al.*, 2002; Bohner and Baroud, 2005). The first CPC was approved in 1996 by the US Food and Drug Administration (FDA) for craniofacial repairs (Friedman *et al.*, 1998). However, because of its low strength, the use of CPC was "limited to the reconstruction of non-stress-bearing bone" (Shindo *et al.*, 1993; Friedman *et al.*, 1998). Applications such as mandibular and maxillary ridge augmentation, major reconstructions of the maxilla or mandible after trauma or tumor resection, and other orthopedic repairs, would be better served with an improved CPC that has fracture resistance and stem cell delivery for rapid bone regeneration. However, while our previous studies have cultured mouse cells with CPC (Weir *et al.*, 2006; Zhao *et al.*, 2010), to date there has been no report on the comparison of hBMSC and hUCMSC encapsulation in CPC.

Therefore, the objective of this study was to encapsulate hUCMSCs and hBMSCs in reinforced CPC scaffolds for bone tissue engineering. Three hypotheses were tested: (1) A stem-cell-encapsulating CPC-fiber construct can achieve the mechanical strength of cancellous bone; (2) hUCMSCs and hBMSCs encapsulated in CPC scaffold will osteo-differentiate and synthesize bone minerals *in vitro*; and (3) hUCMSCs encapsulated in the scaffold will synthesize more bone minerals than the gold-standard hBMSCs.

MATERIALS & METHODS

CPC consisted of tetracalcium phosphate [TTCP: $Ca_4(PO_4)_2O$] and dicalcium phosphate-anhydrous (DCPA: $CaHPO_4$) mixed at a molar ratio of 1:1. Chitosan and its derivatives are natural biopolymers that are biodegradable and osteoconductive (Muzzarelli *et al.*, 1993). Chitosan lactate (referred to as chitosan; Vanson, Redmond, WA, USA) was mixed with water at a chitosan/(chitosan+water) mass fraction of 15% to form the CPC liquid (Xu and Simon, 2005). An absorbable polyglactin fiber (Vicryl, Ethicon, Somerville, NJ, USA) was cut to 8-mm filaments and mixed with CPC at a fiber volume fraction of 20% to reinforce CPC. The paste was filled into 3 x 4 x 25 mm^3 molds, incubated at 37ºC in a humidor for 4 hrs to set, and then de-molded and immersed in water at 37ºC for 20 hrs. The specimens were then tested in three-point flexure on a Universal Testing Machine (5500R, MTS, Cary, NC, USA) to measure flexural strength, elastic modulus, and work-of-fracture (toughness) (Xu *et al.*, 2006).

The use of human stem cells was approved by the University of Maryland Institutional Review Board. hUCMSCs, generously provided by Dr. M.S. Detamore (University of Kansas, Lawrence, KS, USA), were harvested as described previously (Bailey *et al.*, 2007). Cells were cultured in a low-glucose Dulbecco's modified Eagle's medium with 10% fetal bovine serum and 1% penicillin/streptomycin (Invitrogen, Carlsbad, CA, USA), referred to as control media. The osteogenic media for hUCMSCs had 100 nM dexamethasone, 10 mM β-glycerophosphate, 0.05 mM ascorbic acid, and 10 nM 1α,25-dihydroxyvitamin (Baksh *et al.*, 2007; Wang *et al.*, 2009; Zhao *et al.*, 2010). For hBMSCs (Lonza, Allendale, NJ, USA), the osteogenic media contained 100 nM dexamethasone, 10 mM β-glycerophosphate, and 0.05 mM ascorbic acid (Benoit *et al.*, 2007; Zhao *et al.*, 2010).

Quantitative real-time reverse-transcription polymerase chain-reaction measurement (qRT-PCR, 7900HT, Applied Biosystems, Foster City, CA, USA) measured cell differentiation. The total cellular RNA on the scaffolds was extracted with TRIzol reagent (Invitrogen) and reverse-transcribed into cDNA with the use of a High-Capacity cDNA Archive kit. Relative expression levels for human alkaline phosphatase and osteocalcin genes were evaluated by the $2^{-\Delta\Delta Ct}$ method (Livak and Schmittgen, 2001).

Cells were encapsulated in alginate hydrogel beads, which were then mixed with CPC to avoid harming the cells. The rationale was that once CPC had set, the beads could dissolve to release the cells, while concomitantly creating macropores. A 1.2% sodium alginate solution was prepared in saline. hUCMSCs and hBMSCs were encapsulated with 1 million cells/mL of alginate solution. Alginate hydrogel beads were formed by extrusion of alginate-cell droplets into a calcium-chloride solution (Weir *et al.*, 2006; Zhao *et al.*, 2010). The droplets cross-linked and formed beads with a mean diameter of 2.2 mm (Weir *et al.*, 2006). The beads were collected and mixed with CPC at beads/(CPC paste + beads) = 50% by volume.

To measure the alkaline phosphatase activity (ALP), we dissolved the cell-encapsulating hydrogel beads by 55 mmol/L sodium citrate bribasic solution (Sigma, St. Louis, MO, USA). A colorimetric p-nitrophenyl phosphate assay kit (Stanbio, Boerne, TX, USA) and a microplate reader were used. ALP was normalized by the DNA content (Moreau and Xu, 2009). For histological staining of cell-synthesized minerals, the beads were harvested from CPC scaffolds. The cell-synthesized minerals emit red fluorescence when stained with xylenol orange (Sigma). Mineral area percentage was calculated as $A_{Mineral}/A_{Total}$, where $A_{Mineral}$ is the area of mineralization (red fluorescence), and A_{Total} is the total area of the field of view of the image.

We used scanning electron microscopy (SEM, JEOL 5300, Peabody, MA, USA) to examine the samples. The cell specimens were rinsed with saline, fixed with 1% glutaraldehyde, subjected to graded alcohol dehydrations, rinsed with hexamethyldisilazane, sputter-coated with gold, and examined in SEM. Minerals synthesized by the cells were examined by x-ray diffraction (XRD). The cultured cell-laden alginate beads were harvested and then dried. The dried powder was analyzed *via* the XRD and compared with a known hydroxyapatite. The XRD patterns were recorded with a powder x-ray diffractometer (Rigaku, Danvers, MA, USA) with graphite monochromatized copper K_α radiation ($\lambda = 0.154$ nm) generated at 40 kV and 40 mA. The data were collected in a continuous scan mode (1° 2θ min^{-1}, step time 0.6 sec, step size 0.01°) and stored in a computer. In addition, a chemical analysis was performed in which the cell-synthesized powder was placed in a 17.5-mM acetic acid solution to dissolve the powder. The calcium [Ca] and phosphate [PO_4] concentrations were measured *via* a
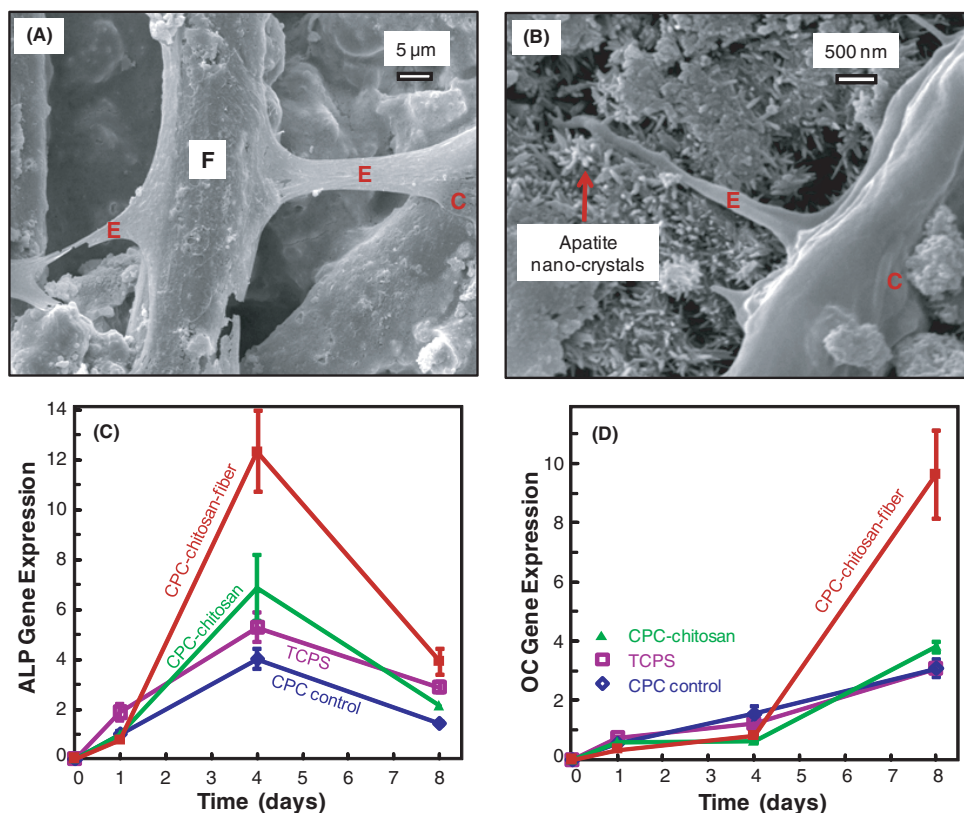
Figure 1. hUCMSC seeding on CPC scaffolds. **(A)** hUCMSCs attached to CPC-chitosan-fiber composite. "C" stands for hUCMSC. "E" refers to the cytoplasmic extensions of the cell. "F" designates polyglactin fiber in CPC. **(B)** hUCMSC extensions attaching to the nano-apatite that makes up the CPC matrix. **(C)** RT-PCR of osteogenic differentiation of hUCMSCs attaching to CPC showed high alkaline phosphatase (ALP) gene expression at day 4. **(D)** Osteocalcin (OC) gene expression peaked at day 8. Each value is the mean of 5 measurements, with the error showing one standard deviation (mean ± SD; n = 5).

mm length, had a flexural strength (mean ± SD; n = 6) exceeding 6 MPa (Fig. 2A) and elastic modulus of 0.9 GPa (Fig. 2B). The work-of-fracture (toughness) was also increased for the CPC-chitosan-fiber scaffold (Fig. 2C).

The hUCMSCs encapsulated inside CPC had a 20-fold increase in ALP at 14 days compared with the control (Fig. 3A). hUCMSCs in CPC control and CPC-chitosan-fiber construct had ALP similar to those in hydrogel without CPC (p > 0.1). This indicates that encapsulation in CPC and the cement-setting reaction did not compromise the hUCMSC viability and osteo-differentiation.

The minerals synthesized by the encapsulated hUC-MSCs were stained *via* xylenol orange. At day 7, little mineral was found (Fig. 3B). The mineral staining area increased at 21 days (Figs. 3C-3E). The mineralization areas for cells inside CPC and CPC-chitosan-fiber constructs were similar to those in hydrogel without CPC. This indicates that encapsulation inside CPC and CPC-chitosan-fiber scaffolds did not compromise the hUCMSCs' mineralization capability compared with those in hydrogel without CPC.

The encapsulated hUCMSCs and hBMSCs were compared for their ability to synthesize bone minerals. The hydrogel contained only 1.2% sodium alginate and 98.8% aqueous solution. Hence, after the harvested beads were dried, there was little material left (after 1 or 7 days of culture), except the substance synthesized by the cells (*e.g.*, at 21 days). The dried substance made by the cells at 21 days had the morphology of minerals (Fig. 4A). XRD patterns of this substance (Fig. 4B) and a known hydroxyapatite (Fig. 4C) had similar peaks in the vicinity of 26° and 32°, confirming that the cell-synthesized substance was apatitic. The peak height was lower for the cell-synthesized mineral, consistent with bio-minerals being low-crystalline (LeGeros, 1993). Chemical analysis of the cell-synthesized substance dissolved in the solution yielded a Ca/P molar ratio of 1.35, which is consistent with the reported Ca/P ratio (between 1.39 and 1.41) of mineral deposited by rat dental pulp cells (Nakamura *et al.*, 2005).

spectrophotometric method (DMS-80 UV-visible, Varian, Palo Alto, CA, USA) with known standards and calibration curves, following previous studies (Vogel *et al.*, 1983).

One-way and two-way ANOVAs were performed to detect significant effects of the variables. Tukey's multiple comparison was used at p = 0.05.

RESULTS

The hUCMSCs readily attached to the CPC-chitosan-fiber scaffold surfaces, anchoring to the fibers (Fig. 1A) and the nano-sized hydroxyapatite crystals in CPC (Fig. 1B). The qRT-PCR results (mean ± SD, n = 5) showed that the ALP gene expression was minimal at day 1; it peaked at day 4, and then decreased at day 8 (C). The OC expression peaked at day 8 (D). At day 4 for ALP and day 8 for OC, the incorporation of fibers into CPC greatly increased the ALP and OC, compared with those without fibers (p < 0.05).

The CPC-chitosan-fiber construct containing the 2.2-mm hydrogel beads with hUCMSCs, as well as Vicryl fibers of 8

The percentage of mineral area (Figs. 4D-4F) (mean ± SD; n = 5) showed that: (1) hUCMSCs made much more mineral than hBMSCs while encapsulated in all 3 constructs (p < 0.05); (2) the mineral amount increased rapidly from 7 to 21 days (p < 0.05); and (3) for the same cell type, encapsulation inside the 3 different constructs yielded similar mineral amount (p > 0.1), indicating that the stronger CPC-chitosan-fiber scaffold did not compromise the stem cell mineralization, compared with the FDA-approved CPC control and the hydrogel without CPC.

DISCUSSION

This study demonstrated for the first time that hUCMSCs encapsulated inside scaffolds were more potent and synthesized much more bone minerals than the gold-standard hBMSCs. Both hUCMSCs and hBMSCs in the self-setting, nano-apatite CPC-fiber scaffold showed excellent viability, osteo-differentiation, and mineralization *in vitro*. Currently, a major focus in orthopedics is to develop injectable systems that can be molded to the shape of the bone cavity and harden *in situ* when injected (Laurencin *et al.*, 1999; Bohner and Baroud, 2005). The advantages include shorter surgical time, avoiding large muscle-retraction, minimizing post-operative pain and scar size, faster recovery, and lower cost. Previous studies showed that CPC could be rendered injectable through a 10-gauge needle, even when the paste contained porogens and chopped fibers (Xu *et al.*, 2006; Burguera *et al.*, 2008). The present study showed that the strength of the hUCMSC-CPC-chitosan-fiber construct was three-fold that of CPC control and matched the reported tensile strength of 3.5 MPa for cancellous bone (Damien and Parsons, 1991). It was much higher than the strength of previous injectable carriers, which was 0.7 MPa for injectable polymeric carrier (Shi *et al.*, 2007), and 0.1 MPa for hydrogels (Kuo and Ma, 2001; Drury *et al.*, 2004). The reported modulus was 0.008 GPa for an injectable polymeric carrier (Shi *et al.*, 2007) and 0.0001 GPa for hydrogels (Kuo and Ma, 2001; Drury *et al.*, 2004). Hence, the much stronger, stem-cell-encapsulating CPC-chitosan-fiber construct may have the potential to deliver stem cells in a wide range of craniofacial and orthopedic applications.

Natural bone consists of an extracellular matrix with nano-sized apatitic minerals and collagen fibers that support bone cell functions. It is advantageous for a synthetic biomimetic scaffold to: (1) contain nano-apatite crystals similar to those in bone, together with fibers to form a matrix that supports cell attachment; (2) have mechanical properties similar to those of bone; and (3) encapsulate and support cells for osteogenic differentiation and bone regeneration. The polyglactin fibers in CPC consisted of individual fibers of 14-μm diameter, braided to form a rough-surfaced bundle with a bundle diameter of about 300 μm. The surfaces of the CPC-chitosan-fiber specimens were noticeably rougher than those of CPC control without fibers. It is possible that the rougher surfaces of the CPC-fiber scaffold facilitated cell attachment and osteo-differentiation, resulting in much higher ALP and OC (Fig. 1). This is consistent with a recent study that showed a dramatic, three-fold greater bone tissue ingrowth in defects containing carbon-nanotube nanocomposite scaffold, compared with control polymer scaffolds
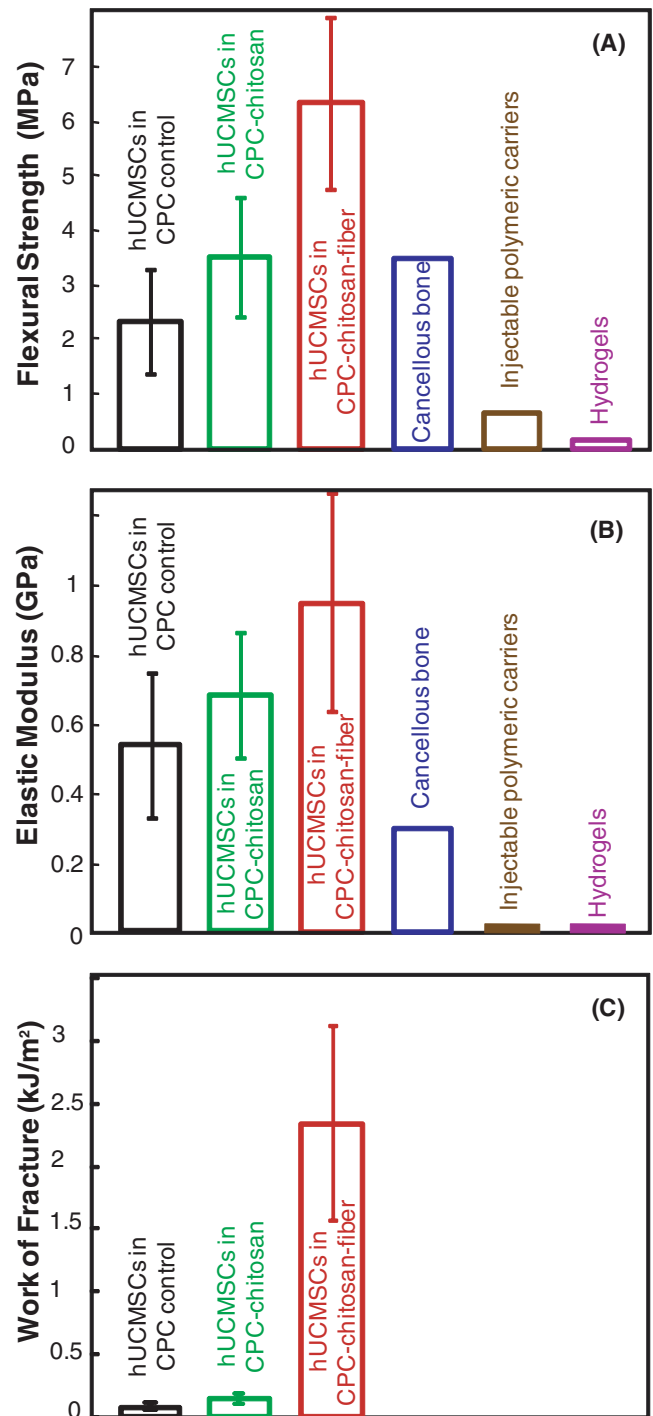

Figure 2. Load-bearing properties. Each specimen contained 50 vol% of alginate hydrogel beads with 150,000 hUCMSCs. The bead diameter was 2.2 mm. The CPC-chitosan-fiber construct was reinforced with Vicryl fibers of 8 mm length. **(A)** The strength of hUCMSC-encapsulating CPC-chitosan-fiber construct was three-fold that of CPC control (mean ± SD; n = 6). It matched the reported tensile strength of 3.5 MPa for cancellous bone (Damien and Parsons, 1991). It was much higher than the strength of previous injectable carriers, which was 0.7 MPa for injectable polymeric carrier (Shi *et al.*, 2007), and 0.1 MPa for hydrogels (Kuo and Ma, 2001; Drury *et al.*, 2004). **(B)** Elastic modulus and **(C)** work-of-fracture of hUCMSC-encapsulating CPC.
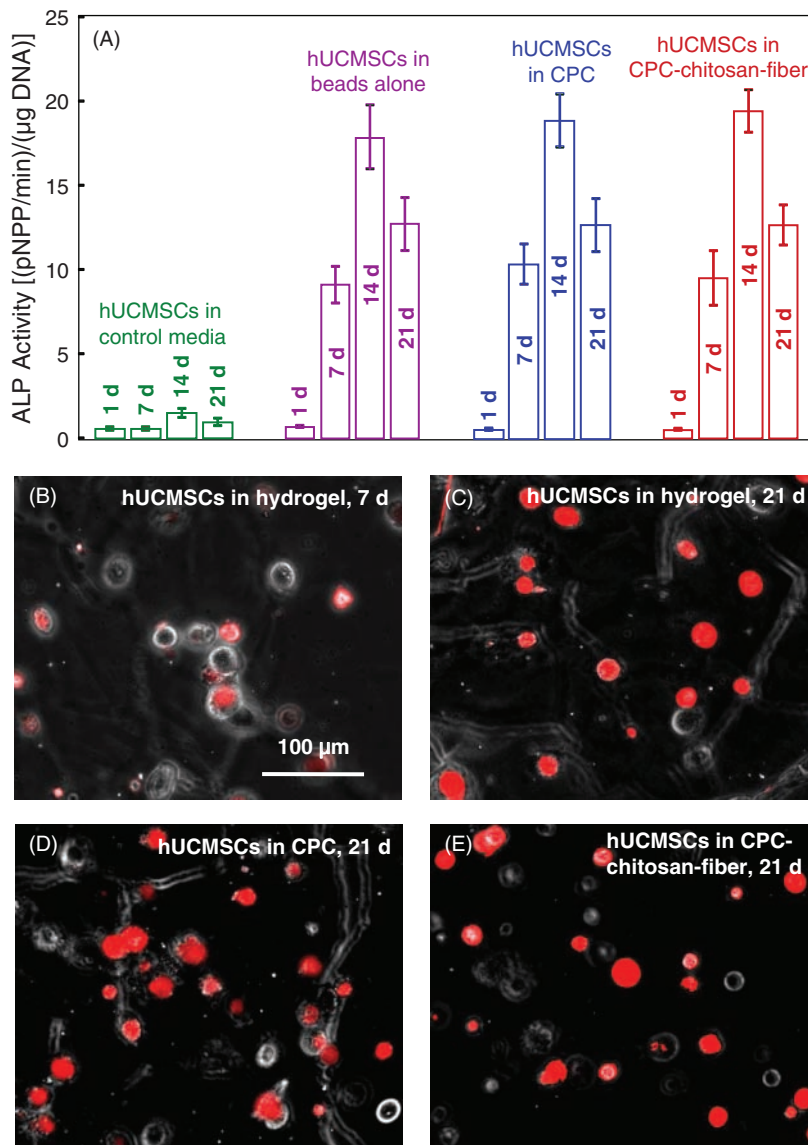
Figure 3. hUCMSC osteo-differentiation and mineralization while encapsulated inside hydrogel beads, inside CPC, and inside CPC-chitosan-fiber scaffold. The bead diameter was 2.2 mm. The fiber length was 8 mm. **(A)** ALP was measured with a p-nitrophenyl phosphate assay (mean ± SD; n = 5). Minerals synthesized by the hUCMSCs were stained by xylenol orange and emitted red fluorescence. **(B)** hUCMSCs in hydrogel at 7 days had minimal mineralization. **(C)** hUCMSCs in hydrogel at 21 days had more mineral. **(D)** hUCMSCs in beads in CPC at 21 days. **(E)** hUCMSCs in CPC-chitosan-fiber scaffold at 21 days.

without nanotubes (Sitharaman *et al*., 2008). This increase was related to the high surface area and roughness that may have enhanced cell attachment and stimulated the cells to synthesize the extracellular matrix. Further study is needed to examine the effects of degradable fibers in CPC on bone formation *in vivo*.

The stem-cell-encapsulating CPC-fiber construct may be promising for dental applications such as mandibular, maxillary, and other craniofacial repairs, as well as for orthopedic applications. For example, combat soldiers have body armor

and solid armor plates to protect their abdomens and chests. However, there is a lack of body armor to protect their faces, where most of the penetrating injuries would occur. Major reconstructions of the maxilla, mandible, and other facial and cranial areas can greatly benefit from a CPC-fiber paste that can be molded to the desired shape for esthetics, with fracture resistance and stem cell encapsulation for rapid bone regeneration. Mandibular and maxillary ridge augmentation would be another ideal use for the stem-cell-CPC construct, as would be the support of metal dental implants or augmentation of deficient implant sites, since these implants would be subject to early loading by provisional dentures and would need to be resistant to flexure. All these dental and craniofacial applications, and a wide range of orthopedic repairs, would potentially be better served with the novel stem-cell-encapsulating and mechanically strong CPC-fiber construct. Animal studies are needed to investigate the bone regeneration efficacy of the CPC-fiber scaffold with stem cell delivery.

In summary, this study encapsulated hUC-MSCs and hBMSCs in strong CPC scaffolds and demonstrated for the first time that hUC-MSCs in scaffolds synthesized more bone minerals than the commonly studied hBM-SCs, which require an invasive procedure to harvest. hUCMSCs and hBMSCs encapsulated in the scaffolds successfully differentiated down the osteogenic lineage, with elevated ALP and synthesis of bone minerals which increased rapidly with time. The stem-cell-encapsulating, self-setting, biomimetic, and mechanically strong construct may find utility in a wide range of dental, maxillofacial, and orthopedic applications, with the potential to greatly enhance bone regeneration. This study showed that the encapsulated hUCMSCs synthesized more bone mineral than the gold-standard hBMSCs, which may have a broad impact on regenerative medicine and dental tissue engineering.

ACKNOWLEDGMENTS

the University of Maryland Dental School.

REFERENCES

Bailey MM, Wang L, Bode CJ, Mitchell KE, Detamore MS (2007). A comparison of human umbilical cord matrix stem cells and temporomandibular joint condylar chondrocytes for tissue engineering temporomandibular joint condylar cartilage. *Tissue Eng* 13:2003-2010.

Baksh D, Yao R, Tuan RS (2007). Comparison of proliferative and multilineage differentiation potential of human mesenchymal stem cells derived from umbilical cord and bone marrow. *Stem Cells* 25:1384-1392.

Barralet JE, Gaunt T, Wright AJ, Gibson IR, Knowles JC (2002). Effect of porosity reduction by compaction on compressive strength and microstructure of calcium phosphate cement. *J Biomed Mater Res* 63:1-9.

Benoit DS, Durney AR, Anseth KS (2007). The effect of heparin-functionalized PEG hydrogels on three-dimensional human mesenchymal stem cell osteogenic differentiation. *Biomaterials* 28:66-77.

Bohner M, Baroud G (2005). Injectability of calcium phosphate pastes. *Biomaterials* 26:1553-1563.

Brown WE, Chow LC (1986). A new calcium phosphate water setting cement. In: *Cements research progress*. Brown PW, editor. Westerville, OH: American Ceramic Society, pp. 352-379.

Burguera EF, Xu HH, Sun L (2008). Injectable calcium phosphate cement: effects of powder-to-liquid ratio and needle size. *J Biomed Mater Res B Appl Biomater* 84:493-502.

Can A, Karahuseyinoglu S (2007). Concise review: human umbilical cord stroma with regard to the source of fetus-derived stem cells. *Stem Cells* 25:2886-2895.

Damien CJ, Parsons JR (1991). Bone graft and bone graft substitutes: a review of current technology and applications. *J Appl Biomater* 2:187-208.

Deville S, Saiz E, Nalla RK, Tomsia AP (2006). Freezing as a path to build complex composites. *Science* 311:515-518.

Drury JL, Mooney DJ (2003). Review. Hydrogels for tissue engineering: scaffold design variables and applications. *Biomaterials* 24:4337-4351.

Drury JL, Dennis RG, Mooney DJ (2004). The tensile properties of alginate hydrogels. *Biomaterials* 25:3187-3199.

Ducheyne P, Qiu Q (1999). Bioactive ceramics: the effect of surface reactivity on bone formation and bone cell function. *Biomaterials* 20:2287-2303.

Foppiano S, Marshall SJ, Marshall GW, Saiz E, Tomsia AP (2004). The influence of novel bioactive glasses on in vitro osteoblast behavior. *J Biomed Mater Res* 71(A):242-249.

Friedman CD, Costantino PD, Takagi S, Chow LC (1998). BoneSource™ hydroxyapatite cement: a novel biomaterial for craniofacial skeletal tissue engineering and reconstruction. *J Biomed Mater Res* 43:428-432.
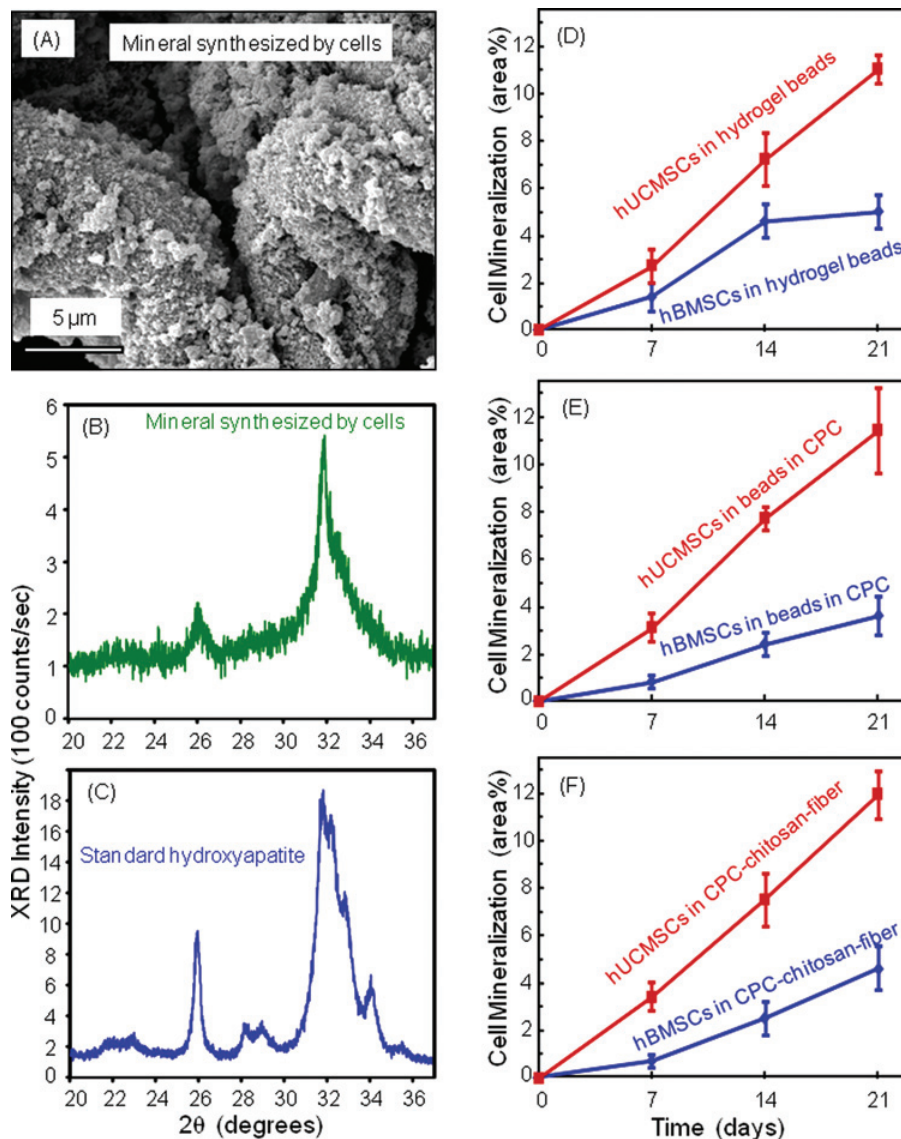
Kuo CK, Ma PX (2001). Ionically crosslinked alginate hydrogels as scaffolds for tissue engineering: Part I. Structure, gelation rate and mechanical properties. *Biomaterials* 22:511-521.

Laurencin CT, Ambrosio AMA, Borden MD, Cooper JA (1999). Tissue engineering: orthopedic applications. *Annual Rev Biomed Eng* 1:19-46.

LeGeros RZ (1993). Biodegradation and bioresorption of calcium phosphate ceramics. *Clin Mater* 14:65-88.

Livak KJ, Schmittgen TD (2001). Analysis of relative gene expression data using real-time quantitative PCR and the $2^{-\Delta\Delta Ct}$ method. *Methods* 25:402-408.

Mao JJ (2008). Stem cells and the future of dental care. *NY State Dent J* 74:20-24.

Figure 4. hUCMSC and hBMSC mineralization. **(A)** SEM of minerals synthesized by the encapsulated hBMSCs at 21 days. **(B)** XRD of minerals by hBMSC at 21 days. **(C)** XRD of a known hydroxyapatite formed at 37°C, provided by Dr. Shozo Takagi at NIST. The XRD patterns confirm that the substance made by the cells was apatitic. **(D-F)** Comparison of mineralization by hUCMSCs and hBMSCs (mean ± SD; n = 5). hUCMSCs synthesized more bone minerals than hBMSCs while encapsulated in all 3 constructs (p < 0.05). Mineralization increased rapidly from 7 to 21 days (p < 0.05).

Mao JJ, Giannobile WV, Helms JA, Hollister SJ, Krebsbach PH, Longaker MT (2006). Craniofacial tissue engineering by stem cells. *J Dent Res* 85:966-979.

Mao JJ, Vunjak-Novakovic G, Mikos AG, Atala A, editors (2007). *Translational approaches in tissue engineering and regenerative medicine*. Boston, MA, USA: Artech House.

Moreau JL, Xu HH (2009). Mesenchymal stem cell proliferation and differentiation on an injectable calcium phosphate-chitosan composite scaffold. *Biomaterials* 30:2675-2682.

Muzzarelli RA, Biagini G, Bellardini M, Simonelli L, Castaldini C, Fratto G (1993). Osteoconduction exerted by methylpyrolidinone chitosan in dental surgery. *Biomaterials* 14:39-43.

Nakamura H, Saruwatari L, Aita H, Takeuchi K, Ogawa T (2005). Molecular and biomechanical characterization of mineralized tissue by dental pulp cells on titanium. *J Dent Res* 84:515-520.

Praemer A, Furner S, Rice DP (1999). *Musculoskeletal conditions in the United States*. Rosemont, IL: American Academy of Orthopedic Surgeons.

Richardson TP, Peters MC, Ennett A, Mooney DJ (2001). Polymeric system for dual growth factor delivery. *Nat Biotechnol* 19:1029-1034.

Shi X, Sitharaman B, Pham QP, Liang F, Wu K, Billups WE, *et al.* (2007). Fabrication of porous ultra-short single-walled carbon nanotube nanocomposite scaffolds for bone tissue engineering. *Biomaterials* 28:4078-4090.

Shindo ML, Costantino PD, Friedman CD, Chow LC (1993). Facial skeletal augmentation using hydroxyapatite cement. *Arch Otolaryngol Head Neck Surg* 119:185-190.

Sikavitsas VI, Bancroft GN, Holtorf HL, Jansen JA, Mikos AG (2003). Mineralized matrix deposition by marrow stromal osteoblasts in 3D perfusion culture increases with increasing fluid shear forces. *Proc Natl Acad Sci USA* 100:14683-14688.

Sitharaman B, Shi X, Walboomers XF, Liao H, Cuijpers V, Wilson LJ, *et al.* (2008). *In vivo* biocompatibility of ultra-short single-walled carbon nanotube/biodegradable polymer nanocomposites for bone tissue engineering. *Bone* 43:362-370.

Vogel GL, Chow LC, Brown WE (1983). A microanalytical procedure for the determination of calcium, phosphate and fluoride in enamel biopsy samples. *Caries Res* 17:23-31.

Wang HS, Hung SC, Peng ST (2004). Mesenchymal stem cells in the Wharton's jelly of the human umbilical cord. *Stem Cells* 22:1330-1337.

Wang L, Singh M, Bonewald LF, Detamore MS (2009). Signaling strategies for osteogenic differentiation of human umbilical cord mesenchymal stromal cells for 3D bone tissue engineering. *J Tissue Eng Regen Med* 3:398-404.

Weir MD, Xu HH, Simon CG (2006). Strong calcium phosphate cement-chitosan-mesh construct containing cell-encapsulating hydrogel beads for bone tissue engineering. *J Biomed Mater Res A* 77:487-496.

Xu HH, Simon CG (2005). Fast setting calcium phosphate-chitosan scaffold: mechanical properties and biocompatibility. *Biomaterials* 26:1337-1348.

Xu HH, Weir MD, Burguera EF, Fraser AM (2006). Injectable and macroporous calcium phosphate cement scaffold. *Biomaterials* 27:4279-4287.

Zhao L, Weir MD, Xu HH (2010). Human umbilical cord stem cell encapsulation in calcium phosphate scaffolds for bone engineering. *Biomaterials* 31:3848-3857.